Ancient DNA and dating evidence for the dispersal of hippos into central Europe during the last glacial

Highlights

- First paleogenome and partial mitogenomes from Late Pleistocene hippos from Europe
- Close genetic link between Late Pleistocene European and modern African hippos
- Radiocarbon dating reveals their mid-Weichselian presence in the Upper Rhine Graben
- Low genome-wide diversity suggests a small, isolated population

Authors

Patrick Arnold, Doris Döppes, Federica Alberti, ..., Axel Barlow, Wilfried Rosendahl, Michael Hofreiter

Correspondence

patrickarnold@uni-potsdam.de (P.A.), wilfried.rosendahl@mannheim.de (W.R.), michael.hofreiter@uni-potsdam.de (M.H.)

In brief

Arnold et al. present evidence that Late Pleistocene hippos from the Upper Rhine Graben show close genetic ties to modern African hippos. Although hippos have been thought to have gone extinct around 115 thousand years ago, further radiocarbon dating suggests their presence in central Europe during the last glacial.







Report

Ancient DNA and dating evidence for the dispersal of hippos into central Europe during the last glacial

Patrick Arnold,^{1,16,*} Doris Döppes,² Federica Alberti,^{1,15} Andreas Füglistaler,^{3,14} Susanne Lindauer,⁴ Christian Hoselmann,⁵ Ronny Friedrich,⁴ Irka Hajdas,⁶ Marc Dickinson,⁷ Frank Menger,⁸ Johanna L.A. Paijmans,^{9,10} Love Dalén,^{11,12,13} Daniel Wegmann,^{3,14} Kirsty E.H. Penkman,⁷ Axel Barlow,¹⁰ Wilfried Rosendahl,^{2,4,*} and Michael Hofreiter^{1,*}

¹Evolutionary Adaptive Genomics, Institute of Biochemistry and Biology, University Potsdam, Karl-Liebknecht-Straße 24-25, 14476 Potsdam, Germany

²Reiss-Engelhorn-Museen, Zeughaus, C5, 68159 Mannheim, Germany

³Department of Biology, University of Fribourg, Chemin du Musée 15, 1700 Fribourg, Switzerland

⁴Curt-Engelhorn-Zentrum Archäometrie gGmbH, C4/8, 68159 Mannheim, Germany

⁵Hessisches Landesamt für Naturschutz, Umwelt und Geologie, Dezernat G1 Geologische Grundlagen, Rheingaustraße 186, 65203 Wiesbaden, Germany

⁶Laboratory of Ion Beam Physics, ETH Zurich, Otto-Stern-Weg 5, 8093 Zurich, Switzerland

⁷Department of Chemistry, University of York, York YO10 5DD, UK

⁸Groß-Rohrheim, Germany

⁹Department of Zoology, University of Cambridge, Downing Street, Cambridge CB2 3EJ, UK

¹⁰School of Environmental and Natural Sciences, Bangor University, Bangor, Gwynedd, LL57 2DG, UK

¹¹Swedish Museum of Natural History, Department of Bioinformatics and Genetics, Box 50007, 10405 Stockholm, Sweden

¹²Centre for Palaeogenetics, Svante Arrhenius väg 20c, 10691 Stockholm, Sweden

¹³Department of Zoology, Stockholm University, 10691 Stockholm, Sweden

¹⁴Swiss Institute of Bioinformatics, 1700 Fribourg, Switzerland

¹⁵Present address: Institute of Pathology, Laboratory of Molecular Tumor Pathology, Charitè Universitätsmedizin Berlin, Virchowweg 15, 10117 Berlin, German

16Lead contact

*Correspondence: patrickarnold@uni-potsdam.de (P.A.), wilfried.rosendahl@mannheim.de (W.R.), michael.hofreiter@uni-potsdam.de (M.H.) https://doi.org/10.1016/j.cub.2025.09.035

SUMMARY

Late Pleistocene hippo fossils (Hippopotamus amphibius) from Europe have generally been associated with the last interglacial period (Eemian, 129-115 thousand years ago [kya]). 1-4 As a widely accepted indicator species for temperate climate conditions, it was assumed they went extinct with the onset of the last glacial (Weichselian) around 115 kya.^{2,5} Their origin and relationships to extant African common hippos and the exact age of their extinction in central Europe, however, remain unclear. Here, we address these questions using an integrated approach applied to hippos from the Upper Rhine Graben in central Europe. By sequencing the paleogenome of a European hippo, we reveal its close genetic links to modern hippos from Africa. Six additional partial mitochondrial genomes confirm that European representatives were part of the same, once widespread species that is today restricted to sub-Saharan Africa. Surprisingly, radiocarbon dating shows that hippos were present in central Europe during the middle Weichselian (a period spanning from earlier than 47 kya until ~31 kya), i.e., well into the last glacial. Similar radiocarbon dates for woolly mammoth and woolly rhino fossils from the same sites imply the presence of both faunas during this period. Despite the paleogenome's low coverage, we are able to confidently estimate its genome-wide diversity by recalibrating the sequencing quality scores and assessing post-mortem damage. The low genome-wide diversity recovered suggests that it belonged to a small, isolated population. Overall, our combined data imply that hippos inhabited the Upper Rhine Graben refugium during temperate phases of the middle Weichselian.

RESULTS AND DISCUSSION

The Middle and Late Pleistocene of Europe was dominated by alternating glacial and interglacial periods.⁶ A particularly exotic element of the European interglacial fauna was the hippopotamus.² Hippos colonized Europe from Africa in multiple waves, probably by multiple species of the genus *Hippopotamus*, including the common hippo (*H. amphibius*) that is today restricted to sub-Saharan Africa.^{7–10} During their maximum geographic distribution in Europe, hippos ranged from the British





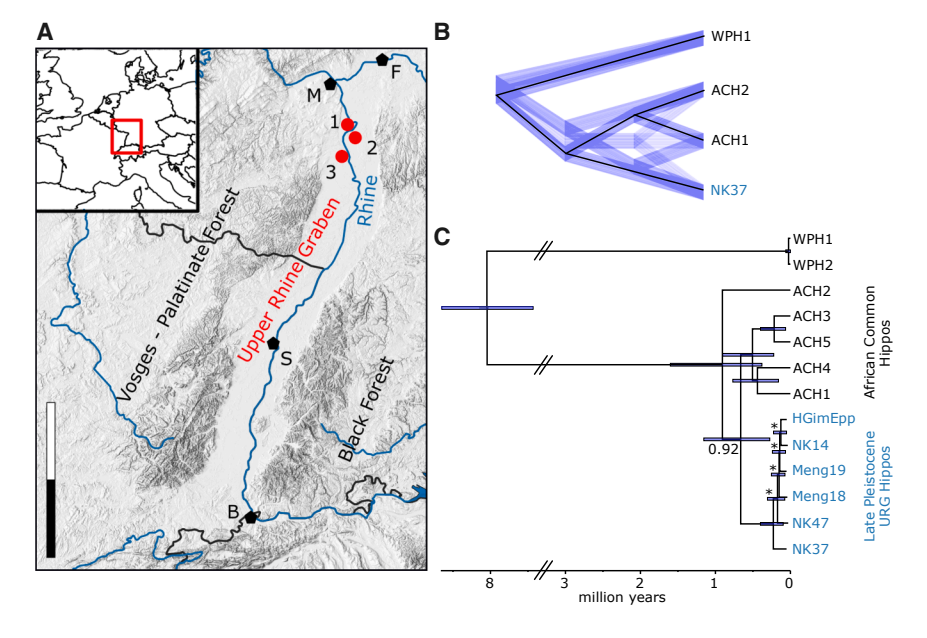


Figure 1. Geographic origin and phylogenetic relationships of fossil hippos from the Upper Rhine Graben

(A) Location of gravel pits in the Upper Rhine Graben (URG) in southwestern Germany where the analyzed fossils of hippos, mammoths, and woolly rhinos have been unearthed (red dots): 1, Gimbsheim/Eich; 2, Groß-Rohrheim; 3, Bobenheim-Roxheim. Black pentagons indicate major cities: B, Basel; F, Frankfurt; M, Mainz; S, Strasbourg. Scale: 100 km in total. (B) Nuclear phylogeny based on 3,085 genomic windows (with uniform branch lengths), including a single ancient sample (NK37) from the URG. Maximum-likelihood tree from concatenated dataset in black (100% bootstrap support), densitree visualization of incongruence among window trees in blue (with uniform branch lengths).

(C) Calibrated Bayesian phylogeny of mitochondrial genomes from Late Pleistocene URG hippos, extant African common hippos (ACH), and extant West African pygmy hippos (WPH) using a Bayesian skyline coalescent tree prior. Node support (posterior probability) is >0.99 for all nodes except those indicated differently or marked with an asterisk (<0.75).

See also Figures S1 and S2 and Table S1.

Isles in the northwest to the Iberian and Italian peninsulas in the south.8 Their presence in the fossil record generally implies temperate conditions with denser vegetation and open water bodies. Hence, it is a widely accepted indicator species for interglacial periods. 1-4 Accordingly, it is generally assumed that both its peak prevalence and maximum geographic distribution in Late Pleistocene Europe coincide with the Eemian interglacial between 129 and 115 thousand years ago (kya) (corresponding to marine oxygen isotope stage [MIS] 5e^{2-4,8}). The onset of cooling at the beginning of the subsequent last glaciation (Weichselian glaciation; 115-11.7 kya; corresponding to MIS 5d-2) consequently led to unfavorable conditions resulting in its extinction in western and central Europe.^{2,5} Their origin and relationships to extant African common hippos (ACHs) and the exact age of their extinction in central Europe, however, still remain unclear, as, beyond morphological identification, only a few detailed analyses have been performed on Late Pleistocene hippos, and ancient DNA data are notably absent for this species.

Close genetic links between Late Pleistocene European and extant African hippos

We subjected 19 hippo specimens from fossil localities in the Upper Rhine Graben in southwestern Germany to paleogenetic analysis (Figure 1A; Table S1). The Upper Rhine Graben represents the easternmost boundary of *Hippopotamus'* Late Pleistocene distribution in central Europe. The long history of quarrying activities in the sandy-gravelly deposits (Mannheim formation see STAR Methods for further details) unearthed numerous fossils of large mammal remains from the Late Pleistocene. As these deposits include representatives from both interglacial and glacial fauna, they have traditionally been interpreted as preserving the transition between the Eemian interglacial and the early Weichselian glacial (MIS4) in central Europe 1-4,12-14 and thus as evidence supporting the hypothesis that hippos went extinct at the end of the Eemian interglacial.

Out of 19 analyzed samples, one (NK37 from the gravel pit Eich; Table S1) yielded a higher proportion of endogenous DNA and was sequenced to $\sim 0.5 \times$ genomic coverage to elucidate phylogenetic relationships between Pleistocene European and extant ACHs. Post-mortem damage patterns support the authenticity of ancient mapped reads (Figure S1). A maximumlikelihood phylogenetic reconstruction, based on 3,085 concatenated 5 kb genomic windows sufficiently covered by paleogenetic data, places the Upper Rhine Graben hippo sample NK37 closer to the two extant ACHs (ACH1 and ACH2) than to the extant West African pygmy hippo (WPH) (Choeropsis liberiensis), which was inferred as a distantly related outgroup (Figure 1B). However, the exact placement of NK37 in regard to the ACH specimens is unclear. The concatenated dataset as well as 44% of window trees place NK37 as sister lineage to both ACH1 and ACH2, but 38% and 18% of window trees support a closer relationship of NK37 to ACH1 or ACH2, respectively (i.e., sample NK37 inside ACHs; Figure 1B). This is further supported by D-statistics (Z = -5.77) that imply a closer relationship of sample NK37 to ACH1 than to ACH2. The discordance could stem from incomplete lineage sorting combined with phylogeographic structure in the ancestral African population. Alternatively, it could be the result of admixture between different hippo lineages in Africa or Europe.

Using enrichment by hybridization capture and stringent sequence calling methods, we additionally recovered partial mitogenomes for six Upper Rhine Graben specimens (completeness ranging from 15% to 78%; Table S1). Authenticity of ancient reads is again supported by post-mortem damage patterns (Figure S1). Maximum-likelihood and Bayesian phylogenetic reconstructions suggest that Late Pleistocene hippos from the Upper Rhine Graben are closely related and form a monophyletic lineage that falls within the mitochondrial diversity of extant ACHs (Figures 1C and S2). An approximately unbiased test, however, cannot exclude (p = 0.131) a position outside

Report



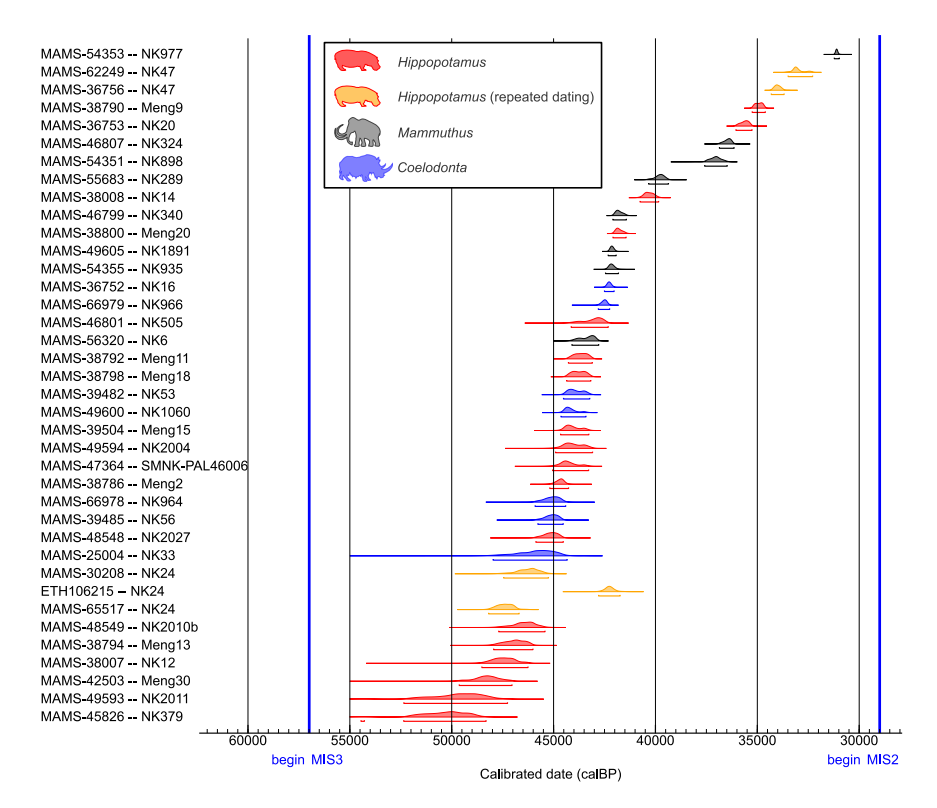


(Figure S3). 28 out of 32 fossil hippo specimens selected for ¹⁴C analysis yielded enough collagen to be dated successfully. The analysis resulted in calibrated dates from the dating limit of ≥49 cal kya BP to as young as 31 cal ky aBP (Figure 2; Table S2). Repeated dating for two samples (including in a second lab) confirmed their young age (Figure 2). Although exact calendar ages have to be interpreted carefully in this time period, our results suggest that hippos were—in contrast to previous assumptions—present in central Europe into the middle of the last glacial period similar to straight-tusked elephants. ^{17,18}

extant ACHs (similar to the main topology in the nuclear concatenation analysis above). Thus, the exact branching order at the beginning of the H. amphibius divergence cannot unambiquously be resolved. The close genetic link of Pleistocene hippos from the Upper Rhine Graben to extant ACHs is also supported by haplotype networks based on a larger, continent-wide sample of mitochondrial cytochrome B (854 nt) and control region sequences¹⁵ (927 nt; Figure S2). In all networks, Pleistocene hippos from the Upper Rhine Graben share haplotypes with specimens mostly known from eastern and southeastern Africa. Mitochondrial distance among contemporary ACHs from different regions in Africa is likewise larger than between Pleistocene hippos and some extant east African hippo lineages. These results show that these Late Pleistocene hippos from Europe do not form a divergent lineage but were part of the once widely distributed common hippo that is now confined to sub-Saharan Africa.

Middle Weichselian presence of hippos in central Europe

Given that their Eemian provenance is solely based on the assumption that hippos are indicative of interglacial conditions in Europe, we next evaluated the age of fossil specimens from the Upper Rhine Graben gravel pits by radiocarbon dating. Samples were collected from deeper layers within each bone to mitigate any bias due to the potential presence of conservatory chemicals that may have been used to treat the surface of fossil specimens for preservation (systematically tested previously ¹⁶). Additionally, Fourier transform infrared (FTIR) spectroscopy indicates that the collagen spectra closely resemble those of reference collagen, suggesting good preservation and purity

Figure 2. Temporal distribution of radiocarbon-dated fossil hippos, mammoths, and woolly rhinos from the Upper Rhine Graben

Probability distributions of radiocarbon dates for fossil hippos (*Hippopotamus*, red), woolly mammoths (*Mammuthus*, gray), and woolly rhinos (*Coelodonta*, blue). Repeated estimates for two hippo specimens (NK47 and NK24) in orange. Estimates for eight additional hippos were beyond the limit of radiocarbon dating (>49 kya). Blue lines mark the boundaries of MISs.

See also Figure S3 and Table S2.

during MIS3, i.e., well into the middle of the last glacial period (middle Weichselian), similar to straight-tusked elephants. 17,18 For comparison, 15 fossils of woolly mammoth (Mammuthus primigenius) and woolly rhino (Coelodonta antiquitatis) from the same or geographically close localities in the Upper Rhine Graben were subjected to ¹⁴C analysis, too. Their estimated dates similarly range between 47 and 31 cal kya BP, and there is no temporal separation between them and hippos (Figure 2: Table S2). To test this further, enamel-based amino acid geochronology was undertaken on three hippo specimens from Eich. The results are not inconsistent with a post-Eemian age for the hippos; however, assigning a definitive MIS3 age is not possible due to the lower temporal resolution of this method for this period (see STAR Methods and Figure S3). Besides hippos, Upper Rhine Graben gravel pits also yielded several other species usually associated with temperate (i.e., interglacial) conditions but without any taphonomic differences to fossils from cold-adapted species that could indicate large-scale temporal differences (e.g., Eemian vs. MIS3; see STAR Methods and Figure S3). This interpretation fits with the absence of sediment layers of Eemian age in the Upper Rhine Graben (see STAR Methods). Together, the dating analyses suggest that, during MIS3, hippos either were broadly contemporaneous with large mammals generally accepted as cold-adapted or, more likely, that hippos and woolly mammoths/rhinos may have cyclically alternated in the Upper Rhine Graben on a short temporal scale not resolvable by our data. This would imply repeated short-term colonization of the Upper Rhine Graben by hippos, for instance, during interstadials (although our radiocarbon dating results do not allow assignment of the hippo fossils to precise interstadials). In either case, Late Pleistocene fossil localities in the Upper



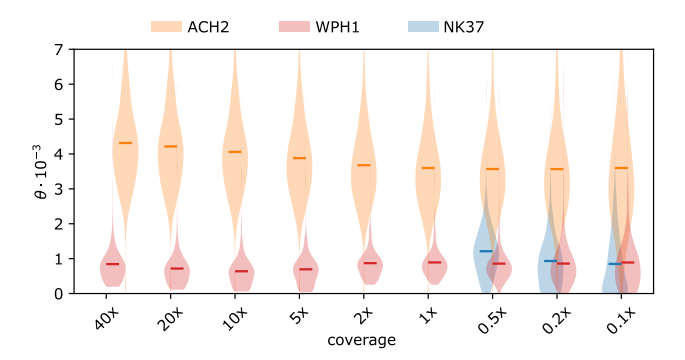


Figure 3. Genome-wide heterozygosity (θ) across different genomic coverage

Estimates for one African common hippo (ACH2), one West African pygmy hippo (WPH1), and the late Pleistocene Upper Rhine Graben sample NK37. Stepwise down-sampling of genomic coverage from original data (left) to as low as $0.1\times$. Results suggest estimates to be robust even down to $0.1\times$ coverage. See also Figure S1 and Table S1.

Rhine Graben seem not to preserve the Eemian interglacial—Weichselian glacial transition.

While hippo presence in central Europe during MIS3 might be surprising, it is not implausible or unlikely. The middle Weichselian is known for its interstadial complex, which includes multiple short interstadial phases resulting in the stagnation of inland ice shield growth. 19-21 The published pollen record from the Upper Rhine Graben and surrounding lower mountain regions shows evidence of plants indicative of temperate, partly forested conditions during MIS3 interstadials.²²⁻²⁹ To provide further support for this, we obtained radiocarbon dates of fossil wood pieces from gravel pits geographically close to those the hippo samples originated from. The dates confirm the presence of cold- (pine) and temperate-associated (oak) tree species in the Upper Rhine Graben during MIS3 (Table S2). Previous analyses from sediments and invertebrate remains similarly suggest multiple warm phases during this period. 30-33 Altogether, the Upper Rhine Graben offered a localized microclimate during several phases of MIS3 that was favorable for sheltering species that require more temperate conditions with relatively mild temperatures. These conditions would have been sufficient to prevent the complete freezing of water bodies and to provide enough vegetation cover for foraging hippos (and likely other temperate-associated species) also during winter. The Upper Rhine Graben might represent the easternmost region with such climate conditions that were suitable for hippo survival and potentially the only one in central Europe during MIS3, as hippos did not spread farther to the east during the Late Pleistocene.^{3,4,8} At the end of MIS3, interstadials were much less common, and the lack of interstadials at the transition to the last glacial maximum¹⁹⁻²¹ likely led to the final extinction of hippos from central Europe.

A small population colonized the Upper Rhine Graben

Radiocarbon ages of the fossil hippos allowed us to further trace the origin of these late-surviving hippos from the Upper Rhine Graben. We performed Bayesian temporal calibration with the mitogenome dataset, associated tip dates, and two tree prior models that both have been shown to best accommodate for mixed inter- and intraspecific sampling.³⁴ Using a Bayesian skyline coalescence tree prior, the basal node within African-European H. amphibius was dated to 834 kya (95% highest posterior density [HPD] 380 kya-1.6 million years ago; Figure 1C). The earliest coalescence among hippos from the Upper Rhine Graben was estimated to 228 kya (95% HPD 96-400 kya). Applying a birth-death tree prior resulted in similar median values for the respective node ages (948 and 242 kya, respectively) but broader HPDs (Figure S2). These divergence dates were also similar when only the three Upper Rhine Graben samples with higher mitogenome completeness (>60%) were included (Figure S2). The basal coalescence within H. amphibius broadly coincides with a period of initial intraspecific diversification and geographic expansion in the ACH as previously shown by molecular and paleontological evidence. 15,35-38 The coalescence among Late Pleistocene hippos from the Upper Rhine Graben provides a genetic proxy for the colonization and expansion in Europe. The temporal range of this node fits with the oldest putative fossils of H. amphibius in Europe from Middle Pleistocene deposits in Italy dating to $\sim\!450$ kya or younger. 10,39,40 Hippos spread across western and central Europe during subsequent interglacial periods, probably using the larger Rhône and Rhine rivers as major routes of dispersal. 1,2 Their presence in central and western Europe during the Holsteinian and Aveley interglacials, however, is disputed, and a definitive fossil record of H. amphibius did not emerge before the Eemian. 1,41 Whether hippos were also present in the Upper Rhine Graben and central Europe in general during the cold periods of the early Weichselian (MIS4) remains unknown but seems unlikely given the near lack of interstadials between 60 and 70 kya. 21 Nevertheless, hippo fossils dating to MIS4 (and potentially younger) are known from the Iberian⁴² and Italian peninsulas, ¹⁰ which might have been the source for the Upper Rhine Graben population in central Europe during the middle Weichselian (MIS3). Eemian and middle Weichselian presence of hippos in western and central Europe thus likely represent different expansion events from southern European refugial areas.

This colonization of the Upper Rhine Graben in central Europe during MIS3 then likely imported the deep mitogenetic lineages (>200 kya) from longer persisting source populations in southern Europe. Such patterns of genetically divergent lineages in close spatial and temporal proximity resemble those seen in other Late Pleistocene mammals in central and western Europe, such as giant deer, woolly rhinoceros, and mammoth, 43-45 and might be the result of periodical colonization of central Europe.⁴⁶ We further evaluated the genetic status of this late-colonizing population by inferring genome-wide diversity in the NK37 paleogenome. Based on post-mortem damage patterns and X chromosome-based recalibration, heterozygosity (θ) was estimated in 5 Mb windows across all autosomes for the nuclear dataset above (Figure S1). Despite the low coverage (0.47×) of the Upper Rhine Graben sample NK37, heterozygosity estimates were robust even when down-sampled to 0.1× coverage (Figure 3). Estimates in the sample NK37 ($\theta_{mean} = 0.00121$) and the WPH1 $(\theta_{mean}$ = 0.000843) are considerably lower than in the two ACHs (ACH1 θ_{mean} = 0.00486; ACH2 θ_{mean} = 0.00431). Extant WPHs are today restricted to the Upper Guinea Forest of western Africa and are fragmented into isolated populations.⁴⁷ The similarly low genome-wide heterozygosity estimated from the



sample NK37 thus suggests that hippos from the Upper Rhine Graben also represented a small, isolated population. 48–50

Conclusions

Middle and Late Pleistocene climate fluctuations resulted in fundamental changes of the environment and its inhabiting large mammal fauna. ^{5,12,51} Glacial and interglacial faunas alternately colonized this area during favorable climate conditions from their core areas in northeastern and southern Europe, respectively, when climate conditions were favorable for them. Nevertheless, neither the timing of colonization and extinction in central Europe nor the phylogenetic relationships to their African relatives could be resolved until now for Late Pleistocene hippos, although they were assumed to be the prime indicator of interglacial conditions.

Here, we approached this issue by combining paleogenomics with radiocarbon dating of putative Eemian hippos from the Upper Rhine Graben. These turned out to be part of the previously much more widely distributed extant ACH, although genomewide data for more Pleistocene European as well as extant ACHs will be needed to disentangle their complex relationships. Contrary to the traditionally accepted view, our newly dated bone remains reveal that hippos did not disappear in central Europe at the end of the Eemian as previously thought. A small population instead recolonized the central European Upper Rhine Graben during MIS3, likely from southern Europe. We thus could show that interstadial phases provided a temperate refugium allowing an (at least temporary) immigration of hippos (and likely other interglacial elements) in the middle of the last glacial period. Overall, the late presence of hippos in the Upper Rhine Graben suggests that fossils from other putative Eemian sites should be re-analyzed as well to evaluate if this species also survived into the last glacial elsewhere in western and central Europe (e.g., the Netherlands⁵²).

RESOURCE AVAILABILITY

Lead contact

Further information and requests for resources and reagents should be directed to and will be fulfilled by the lead contact, Patrick Arnold (patrickarnold@unipotsdam.de).

Materials availability

This study did not generate new, unique reagents.

Data and code availability

- All raw sequencing data produced in this study have been deposited at NCBI Sequence Read Archive (SRA) as BioProject: PRJNA1105865 and are publicly available as of the date of publication. All amino acid data from this study have been deposited at the National Oceanic and Atmospheric Administration (NOAA) repository and are publicly available as of the date of publication (https://www.ncei.noaa.gov/pub/data/paleo/ aar/).
- This paper does not report original code.
- Any additional information required to reanalyze the data reported in this
 paper is available from the lead contact upon request.

ACKNOWLEDGMENTS

This project was conducted within the framework of the research project "Eiszeitfenster Oberrheingraben" ("Ice Age Window Upper Rhine Graben" [2016–2022]), funded by the Klaus Tschira Stiftung GmbH Heidelberg. M.D. and K.E.H.P acknowledge support from the European Union (ERC, EQUATE, 865222). L.D. acknowledges support from the Swedish Research Council

(2021-00625) and the European Union (ERC, PrimiGenomes, 101054984). D.W. acknowledges support from the Swiss National Science Foundation (310030_200420). The authors also acknowledge support from Science for Life Laboratory, the Knut and Alice Wallenberg Foundation, the National Genomics Infrastructure funded by the Swedish Research Council, and the Uppsala Multidisciplinary Center for Advanced Computational Science for assistance with massively parallel sequencing and access to the UPPMAX computational infrastructure. For the purpose of open access, a Creative Commons Attribution (CC BY) license is applied to any author-accepted manuscript version arising from this submission.

AUTHOR CONTRIBUTIONS

Conceptualization, P.A., W.R., and M.H.; methodology, P.A., F.A., D.D., J.L.A.P., A.F., D.W., A.B., W.R., and M.H.; investigation, P.A., F.A., D.D., S.L., C.H., R.F., I.H., M.D., and A.F.; formal analysis, P.A., F.A., D.D., S.L., C.H., R.F., M.D., K.E.H.P., and A.F.; writing – original draft, P.A., D.D., R.F., S.L., C.H., and I.H.; writing – review and editing, P.A., D.D., J.L.A.P., L.D., A.F., D.W., A.B., R.F., W.R., M.D., KE.H.P., and M.H.; resources, D.D., L.D., and W.R.; visualization, P.A., D.D., R.F., and A.F.; and supervision, A.B., W.R., K.E.H.P., and M.H.

DECLARATION OF INTERESTS

The authors declare no competing interests.

STAR*METHODS

Detailed methods are provided in the online version of this paper and include the following:

- KEY RESOURCES TABLE
- EXPERIMENTAL MODEL AND SUBJECT DETAILS
 - Origin of samples and taphonomy
 - Geological setting and stratigraphy
- METHOD DETAILS
 - o Radiocarbon dating
 - o Amino acid geochronology
 - O Ancient DNA laboratory methods
- QUANTIFICATION AND STATISTICAL ANALYSIS
 - O Nuclear genome phylogeny and gene flow
 - Mitochondrial phylogeny and networks
 - o Time-calibrated Bayesian analysis
- Genomic-wide heterozygosity analysis

SUPPLEMENTAL INFORMATION

Supplemental information can be found online at https://doi.org/10.1016/j.cub.2025.09.035.

Received: November 19, 2024 Revised: July 29, 2025 Accepted: September 10, 2025 Published: October 8, 2025

REFERENCES

- Koenigswald, W. von (1988). Paläoklimatische Aussage letztinterglazialer Säugetiere aus der nördlichen Oberrheinebene, Nordteil der Oberrheinebene, and W. von Koenigswald, eds. (Gustav Fischer Verlag), pp. 205–314.
- Von Koenigswald, W. (1991). Exoten in der Großsäuger-Fauna des letzten Interglazials von Mitteleuropa. Quaternary Sci. J. 41, 70–84. https://doi.org/10.3285/eg.41.1.06.
- Koenigswald, W. von (2007). Mammalian faunas from the interglacial periods in Central Europe and their stratigraphic correlation. Dev. Quat. Sci. 7, 445–454.



- van Kolfschoten, T. (2002). The Eemian Mammal Fauna of the Northwestern and Central European Continent (CERP), pp. 21–30.
- Koenigswald, W. von (2003). Mode and causes for the Pleistocene turnovers in the mammalian fauna of Central Europe. Deinsea 10, 305–312
- Förster, M.W., and Sirocko, F. (2016). The ELSA tephra stack: Volcanic activity in the Eifel during the last 500,000 years. Glob. Planet. Change 142, 100–107. https://doi.org/10.1016/j.gloplacha.2015.07.012.
- Faure, M. (1985). Les hippopotames quaternaires non-insulaires d'Europe occidentale. Nouv. Arch. Mus. Hist. Nat. Lyon 23, 13–79. https://doi.org/10.3406/mhnly.1985.1058.
- Pushkina, D. (2007). The Pleistocene easternmost distribution in Eurasia of the species associated with the Eemian *Palaeoloxodon antiquus* assemblage. Mamm. Rev. 37, 224–245. https://doi.org/10.1111/j.1365-2907.2007.00109.x.
- Mazza, P. (1991). Interrelations between Pleistocene hippopotami of Europe and Africa. Boll. Soc. Paleontol. Ital. 30, 153–186.
- Mecozzi, B., Iannucci, A., Mancini, M., Tentori, D., Cavasinni, C., Conti, J., Messina, M.Y., Sarra, A., and Sardella, R. (2023). Reinforcing the idea of an early dispersal of *Hippopotamus amphibius* in Europe: Restoration and multidisciplinary study of the skull from the Middle Pleistocene of Cava Montanari (Rome, central Italy). PLoS One 18, e0293405. https://doi.org/10.1371/journal.pone.0293405.
- Gabriel, G., Ellwanger, D., Hoselmann, C., Weidenfeller, M., and Wielandt-Schuster, U.; Heidelberg; Basin; Project Team (2013). The Heidelberg Basin, Upper Rhine Graben (Germany): a unique archive of Quaternary sediments in Central Europe. Quat. Int. 292, 43–58. https:// doi.org/10.1016/j.quaint.2012.10.044.
- Koenigswald, W. von (2011). Discontinuities in the faunal assemblages and early human populations of Central and Western Europe during the Middle and Late Pleistocene. In Continuity and Discontinuity in the Peopling of Europe, S. Condemi, and G.C. Weniger, eds. (Springer), pp. 101–112. https://doi.org/10.1007/978-94-007-0492-3_9.
- Koenigswald, W. von, and Heinrich, W.-D. (1999). Mittelpleistozäne Säugetierfaunen aus Mitteleuropa-der Versuch einer biostratigraphischen Zuordnung. Kaupia 9, e112.
- 14. Schweiss, D. (1988). Jungpleistozäne Sedimentation in der nördlichen Oberrheinebene. Zur Paläoklimatologie des letzten Interglazials im Nordteil der Oberrheinebene. Paläoklimaforschung 4, 19–78.
- Stoffel, C., Dufresnes, C., Okello, J.B.A., Noirard, C., Joly, P., Nyakaana, S., Muwanika, V.B., Alcala, N., Vuilleumier, S., Siegismund, H.R., et al. (2015). Genetic consequences of population expansions and contractions in the common hippopotamus (*Hippopotamus amphibius*) since the Late Pleistocene. Mol. Ecol. 24, 2507–2520. https://doi.org/10. 1111/moc.12170
- 16. Lindauer, S., Knipper, C., Döppes, D., Knapp, H., Friedrich, R., and Rosendahl, W. (2022). Investigating cave bear remains – an overview on methods with focus on radiocarbon dating and stable isotopes. e-Research Reports of Museum Burg Golling 2, 1–20.
- Mol, D., de Vos, J., and van der Plicht, J. (2007). The presence and extinction of Elephas antiquus Falconer and Cautley, 1847, in Europe. Quat. Int. 169–170, 149–153. https://doi.org/10.1016/j.quaint.2006.06.002.
- Stuart, A.J. (2005). The extinction of woolly mammoth (Mammuthus primigenius) and straight-tusked elephant (Palaeoloxodon antiquus) in Europe. Quat. Int. 126–128, 171–177. https://doi.org/10.1016/j.quaint. 2004.04.021.
- Svensson, A., Andersen, K.K., Bigler, M., Clausen, H.B., Dahl-Jensen, D., Davies, S.M., Johnsen, S.J., Muscheler, R., Rasmussen, S.O., and Röthlisberger, R. (2006). The Greenland ice core chronology 2005, 15– 42 ka. Part 2: comparison to other records. Quat. Sci. Rev. 25, 3258– 3267. https://doi.org/10.1016/j.quascirev.2006.08.003.
- Malmierca-Vallet, I., and Sime, L.C. (2023). Dansgaard–Oeschger events in climate models: review and baseline Marine Isotope Stage 3 (MIS3)

- protocol. Clim. Past 19, 915–942. https://doi.org/10.5194/cp-19-915-2023
- Rasmussen, S.O., Bigler, M., Blockley, S.P., Blunier, T., Buchardt, S.L., Clausen, H.B., Cvijanovic, I., Dahl-Jensen, D., Johnsen, S.J., Fischer, H., et al. (2014). A stratigraphic framework for abrupt climatic changes during the Last Glacial period based on three synchronized Greenland ice-core records: refining and extending the INTIMATE event stratigraphy. Quat. Sci. Rev. 106, 14–28. https://doi.org/10.1016/j.quascirev. 2014.09.007.
- Behre, K.-E. (1989). Biostratigraphy of the last glacial period in Europe.
 Quat. Sci. Rev. 8, 25–44. https://doi.org/10.1016/0277-3791(89) 90019-X.
- Preusser, F. (2004). Towards a chronology of the Late Pleistocene in the northern Alpine Foreland. Boreas 33, 195–210.
- Döppes, D., Rabeder, G., and Stiller, M. (2011). Was the Middle Würmian in the High Alps warmer than today? Quat. Int. 245, 193–200. https://doi. org/10.1016/j.quaint.2011.07.029.
- Sirocko, F., Martínez-García, A., Mudelsee, M., Albert, J., Britzius, S., Christl, M., Diehl, D., Diensberg, B., Friedrich, R., Fuhrmann, F., et al. (2021). Muted multidecadal climate variability in central Europe during cold stadial periods. Nat. Geosci. 14, 651–658. https://doi.org/10.1038/ s41561-021-00786-1.
- Sirocko, F., Albert, J., Britzius, S., Dreher, F., Martínez-García, A., Dosseto, A., Burger, J., Terberger, T., and Haug, G. (2022). Thresholds for the presence of glacial megafauna in central Europe during the last 60,000 years. Sci. Rep. 12, 20055. https://doi.org/10.1038/s41598-022-22464-x.
- 27. Britzius, S., and Sirocko, F. (2023). Vegetation Dynamics and Megaherbivore Presence of MIS 3 Stadials and Interstadials 10–8 Obtained from a Sediment Core from Auel Infilled Maar, Eifel, Germany. Quaternary 6, 44. https://doi.org/10.3390/quat6030044.
- Britzius, S., Dreher, F., Maisel, P., and Sirocko, F. (2024). Vegetation patterns during the last 132,000 years: a synthesis from twelve Eifel Maar sediment cores (Germany): the ELSA-23-Pollen-Stack. Quaternary 7, 8. https://doi.org/10.3390/quat7010008.
- Menzies, J., and Ellwanger, D. (2015). Climate and paleo-environmental change within the Mannheim Formation near Heidelberg, Upper Rhine Valley, Germany: a case study based upon microsedimentological analyses. Quat. Int. 386, 137–147. https://doi.org/10.1016/j.quaint.2015. 03.037
- Moine, O., Antoine, P., Hatté, C., Landais, A., Mathieu, J., Prud'homme, C., and Rousseau, D.D. (2017). The impact of Last Glacial climate variability in west-European loess revealed by radiocarbon dating of fossil earthworm granules. Proc. Natl. Acad. Sci. USA 114, 6209–6214. https://doi.org/10.1073/pnas.1614751114.
- Antoine, P., Rousseau, D.-D., Moine, O., Kunesch, S., Hatté, C., Lang, A., Tissoux, H., and Zöller, L. (2009). Rapid and cyclic aeolian deposition during the Last Glacial in European loess: a high-resolution record from Nussloch, Germany. Quat. Sci. Rev. 28, 2955–2973. https://doi.org/10. 1016/j.quascirev.2009.08.001.
- 32. Fischer, P., Jöris, O., Fitzsimmons, K.E., Vinnepand, M., Prud'Homme, C., Schulte, P., Hatté, C., Hambach, U., Lindauer, S., Zeeden, C., et al. (2021). Millennial-scale terrestrial ecosystem responses to Upper Pleistocene climatic changes: 4D-reconstruction of the Schwalbenberg Loess-Palaeosol-Sequence (Middle Rhine Valley, Germany). Catena 196, 104913.
- Münzing, K., and Stobler, I. (1992). Pleistozäne Mollusken aus Bohrungen im nördlichen Kaiserstuhlvorland. Jahreshefte Geol. Landesamtes Baden Württemb. 34, 395–399.
- Ritchie, A.M., Lo, N., and Ho, S.Y.W. (2017). The impact of the tree prior on molecular dating of data sets containing a mixture of inter-and intraspecies sampling. Syst. Biol. 66, 413–425. https://doi.org/10.1093/sysbio/syw095.
- 35. Okello, J.B.A., Nyakaana, S., Masembe, C., Siegismund, H.R., and Arctander, P. (2005). Mitochondrial DNA variation of the common

Report



- hippopotamus: evidence for a recent population expansion. Heredity 95, 206–215. https://doi.org/10.1038/sj.hdy.6800711.
- Rabinovich, R., and Biton, R. (2011). The Early-Middle Pleistocene faunal assemblages of Gesher Benot Ya 'aqov: inter-site variability. J. Hum. Evol. 60, 357–374. https://doi.org/10.1016/j.jhevol.2010.12.002.
- Klein, R.G., Avery, G., Cruz-Uribe, K., and Steele, T.E. (2007). The mammalian fauna associated with an archaic hominin skullcap and later Acheulean artifacts at Elandsfontein, Western Cape Province, South Africa. J. Hum. Evol. 52, 164–186. https://doi.org/10.1016/j.jhevol. 2006.08.006.
- **38.** Hooijer, D.A., and Singer, R. (1961). The fossil hippopotamus from Hopefield, South Africa. Zool. Meded. *37*, 157–165.
- Martino, R., and Pandolfi, L. (2022). The Quaternary Hippopotamus records from Italy. Hist. Biol. 34, 1146–1156. https://doi.org/10.1080/08912963.2021.1965138.
- Pandolfi, L., and Petronio, C. (2015). A brief review of the occurrences of Pleistocene *Hippopotamus* (Mammalia, Hippopotamidae) in Italy. Geol. Croat. 68, 313–319.
- Schreve, D.C. (2009). A new record of Pleistocene hippopotamus from River Severn terrace deposits, Gloucester, UK—palaeoenvironmental setting and stratigraphical significance. Proc. Geol. Assoc. 120, 58–64. https://doi.org/10.1016/j.pgeola.2009.03.003.
- Fidalgo, D., Madurell-Malapeira, J., Martino, R., Pandolfi, L., and Rosas, A. (2024). An updated review of the Quaternary hippopotamus fossil records from the Iberian Peninsula. Quaternary 7, 4. https://doi.org/10. 3390/quat7010004.
- Rey-Iglesia, A., Lister, A.M., Campos, P.F., Brace, S., Mattiangeli, V., Daly, K.G., Teasdale, M.D., Bradley, D.G., Barnes, I., and Hansen, A.J. (2021). Exploring the phylogeography and population dynamics of the giant deer (*Megaloceros giganteus*) using Late Quaternary mitogenomes. Proc. Biol. Sci. 288, 20201864. https://doi.org/10.1098/rspb.2020.1864.
- Lord, E., Dussex, N., Kierczak, M., Díez-Del-Molino, D., Ryder, O.A., Stanton, D.W.G., Gilbert, M.T.P., Sánchez-Barreiro, F., Zhang, G., Sinding, M.S., et al. (2020). Pre-extinction demographic stability and genomic signatures of adaptation in the woolly rhinoceros. Curr. Biol. 30, 3871–3879.e7. https://doi.org/10.1016/j.cub.2020.07.046.
- Chang, D., Knapp, M., Enk, J., Lippold, S., Kircher, M., Lister, A., MacPhee, R.D.E., Widga, C., Czechowski, P., Sommer, R., et al. (2017). The evolutionary and phylogeographic history of woolly mammoths: a comprehensive mitogenomic analysis. Sci. Rep. 7, 44585. https://doi.org/10.1038/srep44585.
- Hofreiter, M., Serre, D., Rohland, N., Rabeder, G., Nagel, D., Conard, N., Münzel, S., and Pääbo, S. (2004). Lack of phylogeography in European mammals before the last glaciation. Proc. Natl. Acad. Sci. USA 101, 12963–12968. https://doi.org/10.1073/pnas.0403618101.
- Mallon, D., Wrightman, C., De Ornellas, P., Collen, B., and Ransom, C. (2011). Conservation Strategy for the Pygmy Hippopotamus (IUCN Species Survival Commission).
- Spielman, D., Brook, B.W., and Frankham, R. (2004). Most species are not driven to extinction before genetic factors impact them. Proc. Natl. Acad. Sci. USA 101, 15261–15264. https://doi.org/10.1073/pnas. 0403809101
- O'Ryan, C., Harley, E.H., Bruford, M.W., Beaumont, M., Wayne, R.K., and Cherry, M.I. (1998). Microsatellite analysis of genetic diversity in fragmented South African buffalo populations. Anim. Conserv. 1, 85–94. https://doi.org/10.1111/j.1469-1795.1998.tb00015.x.
- Vrijenhoek, R.C. (1994). Genetic diversity and fitness in small populations. In Conservation Genetics, V. Loeschcke, S.K. Jain, and J. Tomiuk, eds. (Springer), pp. 37–53. https://doi.org/10.1007/978-3-0348-8510-2_5.
- Kahlke, R. (1994). Die Entstehungs-, Entwicklungs- und Verbreitungsgeschichtedes oberpleistozänen Mammuthus-Coelodonta-Faunenkomplexes- in Eurasien (Großsäuger). Abh. Senckenberg. Naturforschenden Ges. 546, 1–64.

- Mol, D., and Bakker, R. (2022). Quaternary terrestrial megafaunal remains and their localities in the southern bight of the North Sea between the British Isles and the Netherlands: an overview. Staringia 17, 88–127.
- Gansauge, M.-T., Gerber, T., Glocke, I., Korlević, P., Lippik, L., Nagel, S., Riehl, L.M., Schmidt, A., and Meyer, M. (2017). Single-stranded DNA library preparation from highly degraded DNA using T4 DNA ligase. Nucleic Acids Res. 45, e79. https://doi.org/10.1093/nar/gkx033.
- Martin, M. (2011). Cutadapt removes adapter sequences from highthroughput sequencing reads. EMBnet J. 17, 10–12. https://doi.org/10. 14806/ej.17.1.200.
- Magoč, T., and Salzberg, S.L. (2011). FLASH: fast length adjustment of short reads to improve genome assemblies. Bioinformatics 27, 2957– 2963. https://doi.org/10.1093/bioinformatics/btr507.
- Li, H., and Durbin, R. (2009). Fast and accurate short read alignment with Burrows–Wheeler transform. Bioinformatics 25, 1754–1760. https://doi. org/10.1093/bioinformatics/btp324.
- 57. Li, H., Handsaker, B., Wysoker, A., Fennell, T., Ruan, J., Homer, N., Marth, G., Abecasis, G., and Durbin, R.; Subgroup (2009). Genome Project Data Processing. The sequence alignment/map format and SAMtools. Bioinformatics 25, 2078–2079.
- Korneliussen, T.S., Albrechtsen, A., and Nielsen, R. (2014). ANGSD: analysis of next generation sequencing data. BMC Bioinformatics 15, 356. https://doi.org/10.1186/s12859-014-0356-4.
- 59. Hempel, E., Bibi, F., Faith, J.T., Koepfli, K.-P., Klittich, A.M., Duchêne, D. A., Brink, J.S., Kalthoff, D.C., Dalén, L., Hofreiter, M., et al. (2022). Blue turns to gray: paleogenomic insights into the evolutionary history and extinction of the blue antelope (*Hippotragus leucophaeus*). Mol. Biol. Evol. 39, msac241. https://doi.org/10.1093/molbev/msac241.
- Schliep, K.P. (2011). phangorn: phylogenetic analysis in R. Bioinformatics 27, 592–593. https://doi.org/10.1093/bioinformatics/ htm/706
- 61. Minh, B.Q., Schmidt, H.A., Chernomor, O., Schrempf, D., Woodhams, M. D., Von Haeseler, A., and Lanfear, R. (2020). IQ-TREE 2: new models and efficient methods for phylogenetic inference in the genomic era. Mol. Biol. Evol. 37, 1530–1534. https://doi.org/10.1093/molbev/msaa015.
- Jónsson, H., Ginolhac, A., Schubert, M., Johnson, P.L.F., and Orlando, L. (2013). mapDamage2. 0: fast approximate Bayesian estimates of ancient DNA damage parameters. Bioinformatics 29, 1682–1684. https://doi. org/10.1093/bioinformatics/btt193.
- Larsson, A. (2014). AliView: a fast and lightweight alignment viewer and editor for large datasets. Bioinformatics 30, 3276–3278. https://doi.org/ 10.1093/bioinformatics/btu531.
- Katoh, K., and Standley, D.M. (2013). MAFFT multiple sequence alignment software version 7: improvements in performance and usability.
 Mol. Biol. Evol. 30, 772–780. https://doi.org/10.1093/molbev/mst010.
- Kalyaanamoorthy, S., Minh, B.Q., Wong, T.K.F., von Haeseler, A., and Jermiin, L.S. (2017). ModelFinder: fast model selection for accurate phylogenetic estimates. Nat. Methods 14, 587–589. https://doi.org/10. 1038/nmeth.4285.
- Leigh, J.W., and Bryant, D. (2015). POPART: full-feature software for haplotype network construction. Methods Ecol. Evol. 6, 1110–1116. https://doi.org/10.1111/2041-210X.12410.
- Bouckaert, R., Heled, J., Kühnert, D., Vaughan, T., Wu, C.-H., Xie, D., Suchard, M.A., Rambaut, A., and Drummond, A.J. (2014). BEAST 2: a software platform for Bayesian evolutionary analysis. PLoS Comp. Biol. 10. e1003537. https://doi.org/10.1371/journal.pcbi.1003537.
- Rambaut, A., Drummond, A.J., Xie, D., Baele, G., and Suchard, M.A. (2018). Posterior summarization in Bayesian phylogenetics using Tracer 1.7. Syst. Biol. 67, 901–904. https://doi.org/10.1093/sysbio/syy032.
- Link, V., Kousathanas, A., Veeramah, K., Sell, C., Scheu, A., and Wegmann, D. (2017). ATLAS: analysis tools for low depth and ancient samples. Preprint at bioRxiv. https://doi.org/10.1101/105346.
- Döppes, D., and Rosendahl, W. (2018). The Reiss-Engelhorn-Museen. In Paleontological Collections of Germany, Austria and Switzerland: the



- History of Life of Fossil Organisms at Museums and Universities, L.A. Beck, and U. Joger, eds. (Springer), pp. 411–418. https://doi.org/10.1007/978-3-319-77401-5 41.
- Ziegler, P.A. (1994). Cenozoic rift system of western and central Europe: an overview. Neth. J. Geosci. Geol. Mijnbouw 73, 99–127.
- Ellwanger, D., Gabriel, G., Simon, T., Wielandt-Schuster, U., Greiling, R. O., Hagedorn, E.-M., Hahne, J., and Heinz, J. (2009). Long sequence of Quaternary rocks in the Heidelberg Basin depocentre. E&G Quaternary Sci. J. 57, 316–337. https://doi.org/10.3285/eg.57.3-4.3.
- (2009). The Heidelberg Basin Drilling Project 3/4. In E&G Quaternary Sci. J., 57, G. Gabriel, D. Ellwanger, C. Hoselmann, and M. Weidenfeller, eds., pp. 253–260.
- Hoselmann, C. (2009). The Pliocene and Pleistocene fluvial evolution in the northern Upper Rhine Graben based on results of the research borehole at Viernheim (Hessen, Germany). E&G Quaternary Sci. J. 57, 286–314. https://doi.org/10.3285/eg.57.3-4.2.
- Preusser, F., Büschelberger, M., Kemna, H.A., Miocic, J., Mueller, D., and May, J.-H. (2021). Exploring possible links between Quaternary aggradation in the Upper Rhine Graben and the glaciation history of northern Switzerland. Int. J. Earth Sci. (Geol Rundsch) 110, 1827–1846. https://doi.org/10.1007/s00531-021-02043-7.
- Scheidt, S., Hambach, U., and Rolf, C. (2015). A consistent magnetic polarity stratigraphy of late Neogene to Quaternary fluvial sediments from the Heidelberg Basin (Germany): A new time frame for the Plio-Pleistocene palaeoclimatic evolution of the Rhine Basin. Glob. Planet. Change 127, 103–116. https://doi.org/10.1016/j.gloplacha.2015.01.004.
- Knipping, M. (2008). Early and Middle Pleistocene pollen assemblages of deep core drillings in the northern Upper Rhine Graben, Germany. Neth. J. Geosci. Geol. Mijnbouw 87, 51–65. https://doi.org/10.1017/ S0016774600024045.
- Gegg, L., Jacob, L., Moine, O., Nelson, E., Penkman, K.E.H., Schwahn, F., Stojakowits, P., White, D., Wielandt-Schuster, U., and Preusser, F. (2024). Climatic and tectonic controls on deposition in the Heidelberg Basin, Upper Rhine Graben, Germany. Quat. Sci. Rev. 345, 109018. https://doi.org/10.1016/j.quascirev.2024.109018.
- Lauer, T., Frechen, M., Hoselmann, C., and Tsukamoto, S. (2010). Fluvial aggradation phases in the Upper Rhine Graben—new insights by quartz OSL dating. Proc. Geol. Assoc. 121, 154–161. https://doi.org/10.1016/j. pgeola.2009.10.006.
- Lauer, T., Krbetschek, M., Frechen, M., Tsukamoto, S., Hoselmann, C., and Weidenfeller, M. (2011). Infrared radiofluorescence (IR-RF) dating of middle Pleistocene fluvial archives of the Heidelberg Basin (Southwest Germany). Geochronometria 38, 23–33. https://doi.org/10. 2478/s13386-011-0006-9.
- Kromer, B., Lindauer, S., Synal, H.-A., and Wacker, L. (2013). MAMS-a new AMS facility at the Curt-Engelhorn-Centre for Achaeometry, Mannheim, Germany. Nucl. Instrum. Methods Phys. Res. Sect. B 294, 11–13. https://doi.org/10.1016/j.nimb.2012.01.015.
- Brown, T.A., Nelson, D.E., Vogel, J.S., and Southon, J.R. (1988). Improved collagen extraction by modified Longin method. Radiocarbon 30, 171–177. https://doi.org/10.1017/S0033822200044118.
- Lindauer, S., Tomasto-Cagigao, E., and Fehren-Schmitz, L. (2015). The skeletons of Lauricocha: New data on old bones. J. Archaeol. Sci.: Rep. 4, 387–394. https://doi.org/10.1016/j.jasrep.2015.10.004.
- Reimer, P.J., Austin, W.E.N., Bard, E., Bayliss, A., Blackwell, P.G., Bronk Ramsey, C.B., Butzin, M., Cheng, H., Edwards, R.L., Friedrich, M., et al. (2020). The IntCal20 Northern Hemisphere radiocarbon age calibration curve (0–55 cal kBP). Radiocarbon 62, 725–757. https://doi.org/10. 1017/RDC.2020.41.
- Bronk Ramsey, C. (2001). Development of the radiocarbon calibration program. Radiocarbon 43, 355–363. https://doi.org/10.1017/S00338 22200038212.
- 86. Hajdas, I., Guidobaldi, G., Haghipour, N., and Wyss, K. (2024). Sample selection, characterization and choice of treatment for accurate

- radiocarbon Analysis—Insights from the Eth laboratory. Radiocarbon 66, 1152–1165. https://doi.org/10.1017/RDC.2024.12.
- Dickinson, M.R., Lister, A.M., and Penkman, K.E.H. (2019). A new method for enamel amino acid racemization dating: a closed system approach. Quat. Geochronol. 50, 29–46. https://doi.org/10.1016/j.quageo.2018.11.005.
- Dickinson, M.R., Scott, K., Adams, N.F., Lister, A.M., and Penkman, K.E. H. (2024). Amino acid dating of Pleistocene mammalian enamel from the River Thames terrace sequence: a multi-taxon approach. Quat. Geochronol. 82, 101543. https://doi.org/10.1016/j.quageo.2024. 101543.
- Gibbard, P.L., and Stuart, A.J. (1975). Flora and vertebrate fauna of the Barrington Beds. Geol. Mag. 112, 493–501. https://doi.org/10.1017/ S0016756800046215.
- Gao, C., and Boreham, S. (2011). Ipswichian (Eemian) floodplain deposits and terrace stratigraphy in the lower Great Ouse and Cam valleys, southern England, UK. Boreas 40, 303–319. https://doi.org/10.1111/j.1502-3885.2010.00191.x.
- Lewis, S.G., Ashton, N.M., and Jacobi, R. (2011). Testing human presence during the Last Interglacial (MIS 5e): a review of the British evidence.
 In The Ancient Human Occupation of Britain, N. Ashton, S. Lewis, and C. Stringer, eds. (Elsevier), pp. 125–164. https://doi.org/10.1016/B978-0-444-53597-9 00009-1
- Penkman, K.E.H., Preece, R.C., Bridgland, D.R., Keen, D.H., Meijer, T., Parfitt, S.A., White, T.S., and Collins, M.J. (2011). A chronological framework for the British Quaternary based on Bithynia opercula. Nature 476, 446–449. https://doi.org/10.1038/nature10305.
- Ashton, N., and Lewis, S. (2002). Deserted Britain: declining populations in the British late Middle Pleistocene. Antiquity 76, 388–396. https://doi. org/10.1017/S0003598X00090505.
- 94. Sutcliffe, A.J. (1995). Insularity of the British Isles 250 000–30 000 years ago: the mammalian, including human, evidence. In Island Britain: A Quaternary Perspective. In Geol. Soc. Lond. Spec. Publ., R.C. Preece, ed. (The Geological Society of London), pp. 127–140.
- Nelson, E., White, D., Wheeler, L., Wedel, J., Hoselmann, C., Heggemann, H., Rähle, W., and Penkman, K. (2025). An aminostratigraphy of the northern Upper Rhine Graben, Germany. J. Quat. Sci. https:// doi.org/10.1002/jgs.70004.
- Dabney, J., Knapp, M., Glocke, I., Gansauge, M.-T., Weihmann, A., Nickel, B., Valdiosera, C., García, N., Pääbo, S., Arsuaga, J.-L., et al. (2013). Complete mitochondrial genome sequence of a Middle Pleistocene cave bear reconstructed from ultrashort DNA fragments. Proc. Natl. Acad. Sci. USA 110, 15758–15763. https://doi.org/10.1073/ pnas.1314445110.
- Meyer, M., Kircher, M., Gansauge, M.-T., Li, H., Racimo, F., Mallick, S., Schraiber, J.G., Jay, F., Prüfer, K., De Filippo, C., et al. (2012). A highcoverage genome sequence from an archaic Denisovan individual. Science 338, 222–226. https://doi.org/10.1126/science.1224344.
- Paijmans, J.L.A., Baleka, S., Henneberger, K., Taron, U.H., Trinks, A., Westbury, M.V., and Barlow, A. (2017). Sequencing single-stranded libraries on the Illumina NextSeq 500 platform. Preprint at arXiv. https:// doi.org/10.48550/arXiv.1711.11004.
- Taron, U.H., Paijmans, J.L.A., Barlow, A., Preick, M., Iyengar, A., Drăguşin, V., Vasile, Ş., Ştefan, M.A., and Roblíčková, M. (2021). Ancient DNA from the Asiatic Wild Dog (Cuon alpinus) from Europe. Genes 12, 144. https://doi.org/10.3390/genes12020144.
- Li, H. (2013). Aligning sequence reads, clone sequences and assembly contigs with BWA-MEM. Preprint at arXiv. https://doi.org/10.48550/ arXiv.1303.3997.
- 101. van der Valk, T., Pečnerová, P., Díez-del-Molino, D., Bergström, A., Oppenheimer, J., Hartmann, S., Xenikoudakis, G., Thomas, J.A., Dehasque, M., Sağlıcan, E., et al. (2021). Million-year-old DNA sheds light on the genomic history of mammoths. Nature 591, 265–269. https://doi.org/10.1038/s41586-021-03224-9.



- Dierckxsens, N., Mardulyn, P., and Smits, G. (2017). NOVOPlasty: de novo assembly of organelle genomes from whole genome data. Nucleic Acids Res. 45, e18. https://doi.org/10.1093/nar/gkw955.
- 103. Hoang, D.T., Chernomor, O., Von Haeseler, A., Minh, B.Q., and Vinh, L.S. (2018). UFBoot2: improving the ultrafast bootstrap approximation. Mol. Biol. Evol. 35, 518–522. https://doi.org/10.1093/molbev/msx281.
- 104. Shimodaira, H. (2002). An approximately unbiased test of phylogenetic tree selection. Syst. Biol. 51, 492–508. https://doi.org/10.1080/ 10635150290069913.
- Psonis, N., Vassou, D., Nicolaou, L., Roussiakis, S., Iliopoulos, G., Poulakakis, N., and Sfenthourakis, S. (2022). Mitochondrial sequences of the extinct Cypriot pygmy hippopotamus confirm its phylogenetic placement. Zool. J. Linn. Soc. 196, 979–989. https://doi.org/10.1093/zoolinnean/zlab089.
- 106. Boisserie, J.-R., Suwa, G., Asfaw, B., Lihoreau, F., Bernor, R.L., Katoh, S., and Beyene, Y. (2017). Basal hippopotamines from the upper Miocene of Chorora, Ethiopia. J. Vertebr. Paleontol. 37, e1297718. https://doi.org/10.1080/02724634.2017.1297718.
- Marchi, N., Winkelbach, L., Schulz, I., Brami, M., Hofmanová, Z., Blöcher, J., Reyna-Blanco, C.S., Diekmann, Y., Thiéry, A., Kapopoulou, A., et al. (2022). The genomic origins of the world's first farmers. Cell 185, 1842–1859.e18. https://doi.org/10.1016/j.cell.2022.04.008.
- Kousathanas, A., Leuenberger, C., Link, V., Sell, C., Burger, J., and Wegmann, D. (2017). Inferring heterozygosity from ancient and low coverage genomes. Genetics 205, 317–332. https://doi.org/10.1534/genetics.116.189985.
- Felsenstein, J. (1981). Evolutionary trees from DNA sequences: a maximum likelihood approach. J. Mol. Evol. 17, 368–376. https://doi. org/10.1007/BF01734359.





STAR*METHODS

KEY RESOURCES TABLE

DEACENT OF DECOLIDER	COLIDOR	IDENTIFIED
REAGENT or RESOURCE	SOURCE	IDENTIFIER
Chemicals, peptides, and recombinant proteins		
Guanidine hydrochloride	Roth	Cat# 0037.1
Qiagen MinElute kit	Qiagen	Cat# 28004
Sodium hypochlorite, reagent grade	Sigma Aldrich	Cat# 425044
Sodium hypochlorite 12 % Cl ₂ in aqueous solution	VWR Chemicals	CAS No: 7681-52-9
Hydrochloric acid S.G. 1.18 (~36 %)	Fisher Scientific	CAS No: 7647-01-0
Analytical reagent grade Potassium hydroxide	Fisher Scientific	CAS No: 1310-58-3
Ethylenediaminetetra-acetic acid	VWR Chemicals	CAS No: 60-00-4
HPLC grade Sodium acetate trihydrate	Fisher Scientific	CAS No: 6131-90-4
Sodium azide	VWR Chemicals	CAS No: 26628-22-8
HPLC grade Methanol	Fisher Scientific	CAS No: 67-56-1
0.5 M EDTA (pH=8)	Biosharp	Cat# BL518A
Proteinase K	Promega	Cat# V3021
Zymo-spin V column extension reservoir	Zymo	Cat# C1016-50
AccuPrime Pfx DNA Polymerase	Life Technologies	Cat# 12344024
T4 polynucleotide kinase	New England Biolabs	Cat# M0201L
T4 DNA Polymerase	New England Biolabs	Cat# M0203S
Bst 2.0 DNA polymerase	New England Biolabs	Cat# M0537L
Q5 Hot Start High-Fidelity 2× Master Mix	New England Biolabs	Cat# M0494L-100rxn
NEB buffer 2	New England Biolabs	Cat# B7002S
MyBaits Custom Hybridization Capture kit	Arbor Bioscience	Cat# 300448.v5-ARB
Critical commercial assays		
D1000 Screen Tape (Tapestation2200)	Agilent	Cat# 5067-5582
dsDNA HS Assay Kit (Qubit 2.0)	Thermofisher	Cat# Q32851
Deposited data		
Raw sequencing data	This study	NCBI BioProject: PRJNA986302
Amino acid data	This study	https://www.ncei.noaa.gov/pub/ data/paleo/aar/
Oligonucleotides		
P5 indexing primer: AATGATACGGCGACCACC GAGATCTACACnnnnnnnACACTCTTTCCCTA CACGACGCTCTT	Gansauge et al. ⁵³	Sigma Aldrich
P7 indexing primer: CAAGCAGAAGACGGCA TACGAGATnnnnnnnGTGACTGGAGTTCAG ACGTGT	Gansauge et al. ⁵³	Sigma Aldrich
IS7 amplification primer: ACACTCTTTCCCT ACACGAC	Gansauge et al. ⁵³	Sigma Aldrich
IS8 amplification primer: GTGACTGGAGTTC AGACGTGT	Gansauge et al. ⁵³	Sigma Aldrich
Software and algorithms		
Cutadapt 1.18	Martin ⁵⁴	https://cutadapt.readthedocs.io/en/stable/
Flash 1.2.11	Magoč and Salzberg ⁵⁵	https://ccb.jhu.edu/software/FLASH/
Bwa 0.7.17	Li and Durbin ⁵⁶	https://github.com/lh3/bwa
SAMtools 1.15.1	Li et al. ⁵⁷	https://www.htslib.org/
MarkDupsByStartEnd.jar	N/A	https://github.com/dariober/Java-cafe/ tree/master/MarkDupsByStartEnd

(Continued on next page)



Continued		
REAGENT or RESOURCE	SOURCE	IDENTIFIER
Picard 2.18.29	N/A	https://broadinstitute.github.io/picard/
ANGSD 0.935	Korneliussen et al. ⁵⁸	https://github.com/ANGSD/angsd
Windowtrees 1.0.0	Hempel et al. ⁵⁹	https://github.com/achimklittich/ WindowTrees
Phangorn 2.5.5	Schliep ⁶⁰	https://cran.r-project.org/web/packages/phangorn/index.html
IQTREE 2.0.3	Minh et al. ⁶¹	https://github.com/iqtree/iqtree2
MapDamage 2.1.0	Jónsson et al. ⁶²	https://ginolhac.github.io/mapDamage/
Aliview 1.26	Larsson ⁶³	https://ormbunkar.se/aliview/
NOVOPlasty 4.3.1	Larsson ⁶³	https://github.com/ndierckx/NOVOPlasty
MAFFT 7.130	Katoh and Standley ⁶⁴	https://mafft.cbrc.jp/alignment/server/index.html
ModelFinder	Kalyaanamoorthy et al. ⁶⁵	https://iqtree.github.io/ModelFinder/
PopArt 1.7	Leigh and Bryant ⁶⁶	https://popart.maths.otago.ac.nz/
BEAST 2.7.2	Bouckaert et al. ⁶⁷	https://www.beast2.org/
Tracer 1.5.0.52	Rambaut et al. ⁶⁸	https://github.com/beast-dev/tracer/releases/tag/v1.7.2
TreeAnnotator 2.7.1	N/A	https://beast.community/treeannotator
ATLAS	Link et al. ⁶⁹	https://bitbucket.org/wegmannlab/atlas/ src/master/

EXPERIMENTAL MODEL AND SUBJECT DETAILS

Origin of samples and taphonomy

The faunal remains originate from gravel pits in Eich, Gimbsheim and Bobenheim-Roxheim (all Rheinland-Pfalz), and near Groß-Rohrheim (Hessen) in the Upper Rhine Graben of southwestern Germany (Figure 1). Today, the majority of remains are housed in the "Reis Collection" (Klaus Reis, Deidesheim), which comprises about 15,000 remains collected prior to 1984. Since 2016, the collection has been archived in the Reiss-Engelhorn Museen in Mannheim. Additional faunal remains of this study originate from other museums and collections (Tables S1 and S2). Besides hippos, the faunal assemblages of these sites in the Upper Rhine Graben include several 'interglacial' and 'intermediate' elements (sensu von Koenigswald¹²), including *Panthera spelaea* (cave lion), *Palaeoloxodon* (Elephas) antiquus (straight-tusked elephant), Equus sp. (wild horse), Sus scrofa (wild boar), Bos primigenius (aurochs), Bubalus murrensis (water buffalo), Cervus elaphus (red deer), Capreolus capreolus (roe deer), Megaloceros giganteus (giant deer), Dama dama (fallow deer), Alces alces (elk), Stephanorhinus hemitoechus (steppe rhinoceros), and Stephanorhinus kirchbergensis (forest rhinoceros). No systematic bias regarding breakage, completeness and rolling is observable between hippo and other 'interglacial' species compared to woolly mammoth/woolly rhino and other glacial species (Figure S3).

Geological setting and stratigraphy

The Upper Rhine Graben (Figure 1) is one of the most important rift systems in Europe and offers an outstanding sediment trap where a continuous accumulation and preservation of fossils is documented from the Eocene to the Holocene. 11 The long history of quarrying activities in the sandy-gravelly Upper Rhine Graben deposits (Mannheim formation) unearthed numerous fossils of large mammal remains from the Late Pleistocene. Over the last two decades, our understanding of the Mannheim formation has been revised. The Upper Rhine Graben is a south-southwest to north-northeast striking rift structure that is part of the European Cenozoic Rift System extending from the Mediterranean Sea to the Lower Rhine Embayment.⁷¹ The Upper Rhine Graben can be divided into two parts: a southern part from Basel to Karlsruhe and a northern part from Karlsruhe to Mainz. The differences between the two parts are lateral internal rift-structures with different subsidence. Since the River Rhine acted as the only drainage system that connected the Alps with the North Sea, the Upper Rhine Graben acts as a major sediment trap. Therefore, the Upper Rhine Graben offers unique potential for a continuous sediment accumulation and preservation. Continuous subsidence permitted the accumulation of about 300 m of quaternary sediments in the area west of Heidelberg, the so-called "Heidelberg basin."72 In the northern Upper Rhine Graben, the upper quaternary sediments, sand and gravel deposits alternate with clay layers in between. Aiming to provide a better understanding of the geological evolution of the northern Upper Rhine Graben (especially the Heidelberg basin), and its control by climate change and tectonics, and for the correlation of alpine and north European glacial evolution, the Heidelberg Basin Drilling Project was initiated in 2002. 73 The investigations are primarily based on three newly cored boreholes drilled from 2002 until 2008.



By working on various research boreholes in the northern Upper Rhine Graben, a new lithostratigraphic concept could be developed for the Pliocene and Pleistocene sediments of the northern Upper Rhine Graben. ⁷⁴ Four formations could be defined. ^{11,73} The Mannheim Formation completes this lithological sequence. It has a Middle to Late Pleistocene age and mostly starts with a coarse sediment pulse. Several fluvial aggradation cycles follow. Fine-grained floodplain or overbank deposits are often not preserved. Mass deposits of gravel, cobbles, blocks, and diamictons occur at the graben boundaries and at the entry of the Neckar River into the Upper Rhine Graben. The thickness of the Mannheim Formation varies between a few meters and up to 60 m in the subsidence center of the Heidelberg Basin. The heavy mineral fraction of the fine sands within the Mannheim Formation is characterized by an alpine spectrum with unstable heavy minerals such as garnet, epidote, green hornblende, and alterite. This spectrum also dominates local inputs with stable heavy minerals such as zircon, tourmaline, and rutile. A luminescence age on sediments from a core in Kronau about 20 km south of Heidelberg, outside the Heidelberg Basin, at the transition from the Ludwigshafen to the Mannheim Formation, shows an age of 470 ± 41ka, which is correlated with MIS 12.75 In this location, ages correlated with MIS 10, 8, 6, 4, and 2 were also dated. Thus, up to six accumulation phases could be shown for Kronau. However, this interpretation is based on only a few dates and must be validated with further luminescence dating. Nevertheless, these datings correspond well with magnetostratigraphic studies, 6 according to which the Ludwigshafen and Mannheim Formations can be assigned to the normally polarized Brunhes Chron. In recent decades, a large number of research boreholes have been drilled in the northern Upper Rhine Graben, 11,72 several of them allowing better interpretation of the younger sediments and their respective layers. Various boreholes have also been palynologically analyzed. So far, no sediments from the Eemian period were identified. 11,77,78 Data from optically stimulated luminescence (OLS) dating confirm the lack of Eemian sediments in the Mannheim Formation of the Upper Rhine Graben. 79,80 The upper 33m of sediment cores (fitting with the maximum dredging limit in gravel pits) were deposited during the last glacial period (Weichselian, <60 ka), according to OSL dating. 79

METHOD DETAILS

Radiocarbon dating

Radiocarbon dating was performed at the radiocarbon laboratory of the Curt-Engelhorn-Center Archaeometry (CEZA) in Mannheim by extracting collagen according to a modified Longin extraction from hippopotamus bone and tooth samples as described in detail in Lindauer et al. The pretreatment included organic solvents to remove varnish that was applied to most of the bone material for conservation purposes by the collectors, followed by an acid step to remove carbonates, a base step to remove soluble humic acids, and a final acid step to remove any newly accumulated atmospheric contaminating carbon dioxide. The sample was then gelatinized in hydrochloric acid at pH 3 at 60 °C for 20 hours. The remaining solid material was then removed using an Ezee - Filter (Elkay) before ultrafiltration (Vivaspin Turbo 15) of the collagen to remove short-chained contamination. The sample was then freeze-dried, combusted in an elemental analyzer (MicroCube, Elementar) and graphitized to elemental carbon using in-house or commercially available graphitization systems (AGE3, IonPlus). The graphite was then pressed into a target and measured in a MICADAS-type accelerator mass spectrometer system (AMS). The results were fractionation-corrected (to δ^{13} C=-25 per mil) using the δ^{13} C values measured at the AMS. The conventional radiocarbon dates were calibrated using the calibration curve IntCal2020⁸⁴ and the software OxCal 4.4.

The impact of varnish and conservation chemicals of unknown composition with which the fossil specimens have been treated in historical time has been systematically evaluated previously by the authors. ¹⁶ Additional samples from the Reis collection for which suitable amounts of varnish could be collected were tested here. We removed the upper bone layers and dated the varnish of samples NK37 (hippo; MAMS-47983) and NK25 (cave lion; MAMS-47982) to conventional ¹⁴C ages of 30,011 ± 150 and 36,928 ± 262 years BP, respectively. Those results are comparable to the previously published date for the varnish of NK34 (muskox; MAMS-39641) with a conventional ¹⁴C age of 30,958 +- 203 years BP. ¹⁶ For varnish contamination to significantly affect the ¹⁴C age of the bone material, the varnish chemicals would need to survive the sample pre-treatment, particularly the ultrafiltration step, in large quantities while still producing collagen of good condition. However, since all datable samples yielded visibly identifiable collagen with good collagen yields of above 1% up to 10%, we conclude that only negligible amounts of varnish (if any) might have remained in the extract. In the three samples tested, ¹⁴C dates were always different between varnish and cleaned bone. This indicates significant removal of varnish contamination, especially considering the fact that a number of samples produced infinite ¹⁴C ages.

To ensure the accuracy of dating, the two hippo samples with most material left underwent repeated ¹⁴C testing (Figure 2) at CEZA and the radiocarbon laboratory of ETH Zurich, Switzerland, using the same protocol as above. For NK47, both results (measured at CEZA) show reasonable consistency despite not being identical within their margins of error, yielding conventional ¹⁴C ages of 29,398 +- 117 and 28,690 +- 90 years BP, respectively. NK24 was dated twice at CEZA and once at ETH Zurich, with greater variability compared to NK47. While the CEZA results for NK24 are relatively close to each other (43,833 + 484 years BP and 45,060 + 230 years BP, respectively), the ETH Zurich result is even notably younger (37,975 + 550 years BP). Nevertheless, all dating repetitions confirm the MIS3 age of the hippo fossils. Additional FTIR spectral analysis was conducted on a Spotlight 200i system (PerkinElmer, Waltham, MA, USA) at the ETH laboratory for the sample prepared there following Haijdas et al. ⁸⁶ (Figure S3).

Fossil wood pieces were not covered by lacquer or varnish. They underwent a standard ABA (acid-base-acid) pretreatment with 2M hydrochloric acid (HCl) and 4% sodiumhydroxid (NaOH) followed by 2M HCl again to remove limestone and soluble humic acids. Subsequent steps for graphitization and measurement were the same as described for bone above.



Amino acid geochronology

Three hippo tooth enamel samples from Eich, Upper Rhine Graben, and seven from Barrington, Britain for comparison (Figure S3; Table S2) were prepared using established protocols for intra-crystalline protein analysis of enamel. 87 Enamel chips were mechanically cleaned to remove adhesive residues and non-enamel dental tissues, then powdered and subjected to a 72-hour bleach treatment to isolate the closed-system protein fraction. Each sample was divided into two subsamples: one was analyzed for free amino acids (FAA), while the other was hydrolyzed to determine total hydrolysable amino acids (THAA). Samples were demineralized in HCI before the pH was raised with KOH and the solution centrifuged, producing a biphasic separation; the supernatant was extracted, dried via centrifugal evaporation, and rehydrated in an internal standard. Samples were analyzed in preparative duplicate by reversephase high-performance liquid chromatography, with standards and blanks run alongside. Due to deamination during hydrolysis, aspartic acid and asparagine were recorded together as Asx, and glutamic acid and glutamine as Glx. Racemization ratios of Asx, Glx, phenylalanine, and alanine were used to construct intra-crystalline protein decomposition (IcPD) profiles, exploiting their differential racemization rates for temporal resolution. Comparison of FAA and THAA D/L values were used to assess the extent of closed-system behavior, with significant divergence suggesting possible contamination or diagenetic alteration. To date, no hippopotamus enamel from Germany has been analyzed for its intra-crystalline protein decomposition (IcPD). Consequently, the hippo enamel from Eich has been compared with an established enamel chronology for elephantids (*Palaeoloxodon* and *Mammuthus*) from Britain, 88 as well as a smaller set of British hippo enamel specimens attributed to the Eemian based on the pollen assemblage, optical spin luminescence dates and opercula-based amino acid racemization dating. 89-92 The attribution of H. amphibius remains to MIS5e sites in Britain is therefore likely more robust than on the European mainland, owing to Britain's isolation. 93.6

Differences in the underlying protein sequences between taxa lead to consistently different rates of racemization, limiting direct comparison across species. ⁸⁸ The IcPD values of the Eich hippo enamel were therefore also compared to hippo enamel from a British site (Barrington beds) correlated with the Eemian. As racemization rates are temperature-dependent, regions that experienced a significantly different integrated temperature history will exhibit different rates of IcPD. However, recent opercula-based dating shows that there is only a slight difference in IcPD between last interglacial sites in Britain and near the Upper Rhine Graben on interglacial sediments are directly available from the Upper Rhine Graben), suggesting that the even-slower racemizing enamel from Britain is likely to be comparable to parts of south-western Germany in terms of racemization behavior. As racemization values from the Eich hippo specimens are similar to those of British hippos (Figure S3), a comparison between both geographic regions is valid (within the limitation of taxon-specific differences). When compared to the larger British elephantid time series dataset, the IcPF values of the Eich hippo enamel fall between those samples from MIS4/3 and MIS53 (Eemian), although closer to the former (Figure S3). However, because of the slow rates of racemization in enamel, the confidence intervals of IcPD for MIS4/3 elephantids are relatively large and partially overlap with those of MIS5e elephantids; this is likely to also apply to hippos. Therefore, a post-Eemian age for the Eich hippo samples is possible but cannot currently be confirmed by amino acid racemization dating alone due to the lower temporal resolution of this enamel-based method for this period.

Ancient DNA laboratory methods

All pre-amplification steps were carried out in the dedicated ancient DNA facilities at the University of Potsdam, including negative controls for both extraction and library preparation. In a first round of screening, ~50 mg of bone powder per sample were collected using a Dremel Fortiflex (9100-21) and a 2.4- to 2.8-mm-diameter drill bit. DNA was extracted following a protocol optimized for highly fragmented DNA. 96 A total amount of 13 ng of DNA for each extract was initially treated with USER enzyme for 15 minutes at 37° C (modified from Meyer et al. 97) to remove uracil residues resulting from cytosine deamination. The USER-treated extracts were then converted into single stranded libraries using the protocol described in Gansauge et al. 53 The resulting libraries were then amplified and dual-indexed. PCR cycles for amplification were determined in advance using qPCR analysis of the unamplified library. Concentration and length distribution were determined using Qubit 2.0 and 2200 TapeStation (Agilent Technologies), respectively. The single-stranded libraries were sequenced on an Illumina NextSeq500 system⁹⁸ at the University of Potsdam in 75bp single-end mode for five to 20 million reads. A single sample (NK37) yielded sufficient endogenous DNA to sequence its (non-enriched) library for 3 billion reads on an Illumina NovaSeq6000 system at the SciLifeLab, Stockholm, in 100bp paired-end mode. Libraries were additionally enriched for mitochondrial DNA by two rounds of in-solution hybridization capture using the Arbor Biosciences MyBaits kit according to the manufacturer's instructions (Manual v4.01, April 2018). Enrichment capture baits were designed based on the mitochondrial reference genome of the African common hippo (GenBank: NC_000889.1). Enriched libraries were amplified following the amplification steps used in Taron et al.⁹⁹ and then sequenced again on an Illumina NextSeq500 system at the University of Potsdam in 75bp single-end mode.

QUANTIFICATION AND STATISTICAL ANALYSIS

Nuclear genome phylogeny and gene flow

The nuclear data set consisted of sequencing data for one ancient sample (NK37) and three previously published modern hippos (ACH1, ACH2, WPH1; Table S1). Adapter sequences and low-quality bases (< Q30) were trimmed and reads shorter than 30bp removed with cutadapt 1.18.⁵⁴ Untrimmed reads were discarded. Paired reads were merged with flash 1.2.11.⁵⁵ For NK37, only merged reads were subsequently mapped to the West African pygmy hippo reference genome (GenBank: GCA_023065765.1) using BWA 0.7.17⁵⁶ -aln with relaxed mapping parameter (-n 0.01). Reads with a mapping quality below 30 were removed using Samtools



1.15.1.⁵⁷ Duplicate reads were identified using the java program MarkDuplicatesByStartEnd.jar (https://github.com/dariober/Java-cafe/tree/master/MarkDupsByStartEnd) and removed. For ACH1, ACH2 and WPH1, merged and unmerged reads were mapped to the West African pygmy hippo reference genome (GenBank: GCA_023065765.1) using BWA 0.7.17 -mem.¹⁰⁰ Duplicate reads were identified using Picard 2.18.29 (http://broadinstitute.github.io/picard/). For the sliding window tree analyses, we generated pseudo-haploid sequences using random read sampling (-doFasta 1) in ANGSD 0.935⁵⁸ and the following parameter settings: -minQ 30, -minMapQ 30, -uniqueonly 1, -only_proper_pairs 0, -remove_bads 1, -baq 2, -C 0, -explode 1, -doCounts 1, -trim 0. We ran a sliding window tree analysis⁵⁹ using WindowTrees v1.0.0 (https://github.com/achimklittich/WindowTrees) in binary mode to exclude transitions (-binary), with a missing data threshold of 50% (-N 0.5), a window size of 5kb (-w 5000) and a gap size of 5kb between windows (-lw 5000). Topological incongruence among window trees were visualized as densitree with the phangorn 2.5.5 package⁶⁰ in R. A Maximum Likelihood tree was computed from concatenated windows in IQTREE 2.0.3⁶¹ using the Jukes-Cantor model for binary data. To test for gene flow, D-statistics were calculated using ANGSD 0.935 (-doAbbababa), with WPH1 as outgroup and NK37, ACH1 and ACH2 as P1, P2 and P3, respectively, and the following settings: -doCounts 1, -useLast 1, -rmTrans (use only transversion sites), -minQ 30, -minMapQ 30, -uniqueonly 1, -remove_bads 1, -baq 2, -setMinDepth 3. Standard errors estimation using jackknife procedure was done on block size of 5 Mb. Z-scores >|3| were defined as significant.

Mitochondrial phylogeny and networks

Adapter sequences and low-quality bases (< Q30) were trimmed with cutadapt 1.18. Untrimmed reads were discarded. An individual minimum length cut-off was determined empirically for each library as described previously ¹⁰¹ (Table S1). Trimmed reads were subsequently mapped to the nuclear (GenBank: GCA_023065835.1) and mitochondrial genome (GenBank: NC_000889.1) of the African hippopotamus using BWA aln 0.7.17 with relaxed mapping parameter (-n 0.01). Reads with a mapping quality below 30 were removed using Samtools 1.15.1. Duplicate reads (reads with the same start and end coordinates) were identified using the java program MarkDuplicatesByStartEnd.jar (https://github.com/dariober/Java-cafe/tree/master/MarkDupsByStartEnd) and removed. Cytosine deamination patterns and length distribution of resulting reads were calculated using mapDamage 2.1.0.⁶² (Figure S1.) Mitochondrial consensus sequences were called using Samtools 1.15.1 with 85% majority rule for base calling and minimum coverage of 2x. Consensus calling was also repeated with minimum coverage of 3x. Consensus sequences were manually checked for premature stop-codons in aliview 1.26.⁶³ Mitogenomes of living hippos have either previously been published or were here assembled de-novo from available sequencing data (Table S1). For the latter, paired-end sequencing reads were trimmed with cutadapt 1.18 and assembled with NOVOPlasty 4.3.1¹⁰² with default parameters.

Ancient and modern mitochondrial genomes were aligned using MAFFT v7.310.⁶⁴ Poorly-aligning parts of the D-loop were removed from the alignment resulting in a total alignment length of 16,126 bp. The optimal set of partitions and substitution models under the Bayesian information criterion from all possible combinations of rRNAs, tRNAs and the individual codon positions of protein coding genes was determined using ModelFinder⁶⁵ as implemented in IQTREE 2.0.3. A Maximum Likelihood phylogenetic tree with 1000 ultrafast bootstrap¹⁰³ replications was reconstructed in IQTREE 2.0.3 from the resulting three partition scheme. Results of the phylogenetic reconstruction were consistent using different minimum coverage limits for consensus calling (Figure S2). All subsequent analyses were therefore done with consensus mitogenome sequences with minimum coverage of 2x. The Maximum Likelihood reconstruction was rerun but with constraining Upper Rhine Graben hippos to fall outside all extant African common hippos. The likelihood of both trees (Upper Rhine Graben hippos outside or inside African common hippos) were then compared using the approximately unbiased test¹⁰⁴ as implemented in IQTREE 2.0.3. We additionally used two larger datasets from partial mitochondrial sequences in order to capture the genetic diversity of the extant African common hippo.¹⁵ The first dataset contains 854 bp of cytochrome b from 23 individuals (GenBank: KR005049-KR005071). The second dataset contains 929 bp of tRNA-Pro, the control region and tRNA-Phe from 66 individuals (GenBank: KR004948-KR005044). Respective sequences from Upper Rhine Graben hippos (if preserved) were added to the datasets and minimum-spanning haplotype networks were reconstructed in PopArt 1.7⁶⁶ (Figure S2).

Time-calibrated Bayesian analysis

To estimate the divergence time among late Pleistocene hippos from the Upper Rhine Graben as well as to extant African common hippos, a time-calibrated Bayesian analysis was performed in BEAST 2.7.2⁶⁷ using the same alignment and partition scheme as for the Maximum Likelihood phylogenetic reconstruction above. Pleistocene samples in the alignment were fixed at their above calibrated radiocarbon dates. Samples dated to beyond the radiocarbon limits (>49 ka) were fixed to 59 ka as their presence in the Upper Rhine Graben during MIS4 is unlikely given the near lack of interstadials before 60 ka.²¹ The divergence between *H. amphibius* and *C. liberiensis* was set to 8.1 Ma (normal distribution prior with a mean of 8.1 Ma and a standard deviation of 310 ka) as node calibration following previous estimates.^{105,106} The analysis was run using a Bayesian skyline coalescent tree prior and lognormal relaxed clock models for each partition. As population structuring among and within species may violate the assumptions of the Bayesian skyline coalescent model, the divergence dating analysis was replicated using a Birth-Death speciation tree prior. Both tree prior models, however, have been shown to best accommodate for mixed inter- and intraspecific sampling.³⁴ The MCMC chain was run for 50 million generations. Convergence and adequate sampling (ESS > 200) of all parameters were verified in Tracer 1.5.0.52.⁶⁸ The first 10% of trees were removed as burn-in, and the maximum clade credibility trees obtained from the posterior sample, with node heights scaled to the median of the posterior sample, using TreeAnnotator 2.7.1.



Genomic-wide heterozygosity analysis

Nuclear data sets including NK37, ACH1, ACH2 and WPH1 were processed with the Gaia part of the ATLAS¹⁰⁷ pipeline (bitbucket. org/wegmannlab/atlas-pipeline, commit f3db9e3). For sample NK37, the analysis was restricted to the first mates since most reads did not have a second mate. Reads were trimmed using TrimGalore 0.6.7 (github.com/FelixKrueger/TrimGalore) with no quality filter and a length filter of 30. Reads were subsequently aligned to the African common hippo reference genome (GenBank: GCA 023065835.1) using BWA-mem 0.7.17. Reads with a mapping quality below 30, unmapped and, in the case of paired-end sequencing data, unpaired reads were removed with samtools 1.9. Duplicate reads were marked using MarkDuplicates in picard 2.26.11 (http:// broadinstitute.github.io/picard/). After filtering, a total of 1'845'041'892, 499'769'574, 720'280'245 and 30'909'422 sequencing reads were retained for ACH1, ACH2, WPH1 and NK37, respectively, which resulted in respective average coverages of 75.7x, 39.7x, 42.7x and 0.476x. As expected for ancient samples sequenced with single strand libraries, the sequencing data NK37 showed clear patterns of post-mortem damage at both the 5' and 3' end (Figure S1). Heterozygosity (θ) was estimated from genotype likelihoods as outlined in Kousathanas et al. 108 and implemented in ATLAS⁶⁹ (bitbucket.org/wegmannlab/atlas, commit f1ec7fd), using the functions estimateErrors and theta. In brief, this approach first estimates post-mortem damage patterns and sequencing error rates, which are then used to calculate accurate genotype likelihoods. From these, heterozygosity is subsequently inferred as the rate $\theta = 2T\mu$ under Felsenstein's substitution model. ¹⁰⁹ Error rates were modeled using the following covariates: quality score, position in thread, mapping quality, fragment length and context (i.e. the previous base sequenced). The model was inferred from all sequence data on the X chromosome assuming no heterozygosity as all samples were males. θ was then inferred in 458 5Mb windows along all autosomes. Given their high sequencing quality, diversity estimation in modern samples (ACH1, ACH2, WPH1) were not affected by post-mortem damage and X chromosome-based recalibration (Figure S1). In contrast, they strongly reduce diversity overestimation in NK37 (Figure S1). To confirm the accuracy of the inferred post-mortem damage patterns and sequencing error rates, and consequently of diversity estimates, θ was also inferred from sequencing data down-sampled to 0.5x,0.2x, 0.1x and 0.05x using the task theta with the option -probs. Under accurate estimates of post-mortem damage patterns and sequencing error rates, the diversity estimates are expected to be rather insensitive to the sequencing depth. In case of over- or underestimated sequencing errors, however, the diversity is expected to be under or overestimated, respectively, at low depth. Inferred values of the indeed were robust against down-sampling (at least as low as 0.1x; Figure 3), suggesting that genetic diversity was inferred with high accuracy.